

## Long-term exercise training is associated with unique cardiac troponin I phosphorylation pattern and benign myocardial hypertrophy in the right ventricle in an experimental model of exercise-induced myocardial remodelling

Attila Oláh<sup>a,\*</sup>, Beáta Bódi<sup>b</sup>, Bálint András Barta<sup>a</sup>, Olívía Bottlik<sup>a</sup>, Alex Ali Sayour<sup>a</sup>, Mihály Ruppert<sup>a</sup>, Karolina Katarzyna Kolodziejska<sup>a</sup>, Andrea Kovács<sup>c,d</sup>, Zoltán V. Varga<sup>c,d</sup>, Péter Ferdinandy<sup>c,d,e</sup>, Oliver Schilling<sup>f</sup>, Zoltán Papp<sup>b</sup>, Béla Merkely<sup>a</sup>, Tamás Radovits<sup>a</sup>

<sup>a</sup> Department of Experimental Cardiology and Surgical Techniques, and Department of Cardiology, Heart and Vascular Center, Semmelweis University, Budapest, Hungary

<sup>b</sup> Division of Clinical Physiology, Department of Cardiology, University of Debrecen, Debrecen, Hungary

<sup>c</sup> Center for Pharmacology and Drug Research & Development, Semmelweis University, Budapest, Hungary

<sup>d</sup> Department of Pharmacology and Pharmacotherapy, Semmelweis University, Budapest, Hungary

<sup>e</sup> Pharmahungary Group, Szeged, Hungary

<sup>f</sup> Faculty of Medicine, Institute of Surgical Pathology, University of Freiburg Medical Center, Freiburg, Germany

### ARTICLE INFO

#### Keywords:

Right ventricle  
Athlete's heart  
In vivo electrophysiology  
Contractility  
Physiological hypertrophy

### ABSTRACT

**Background:** Research projects have focused on exercise-induced alterations of the right ventricle (RV) of the heart, because the exercise-associated disproportionate load on the RV might lead to pathological consequences, such as interstitial fibrosis, chamber dilation or pro-arrhythmic remodelling. We aimed at providing a complex characterization of RV alterations induced by regular training in a rat model of exercise-induced cardiac remodelling.

**Methods:** Young, adult rats were divided into control (Co) and exercised (Ex) groups. Exercised rats swam 200 min/day for 12 weeks. In vivo cardiac electrophysiological study and in vitro force measurements on isolated permeabilized RV cardiomyocytes were performed to investigate electrical and functional alterations, respectively. Molecular biological and histological investigations were carried out.

**Results:** Exercise training was associated with mild increased RV hypertrophy (cardiomyocyte diameter:  $12.5 \pm 0.1 \mu\text{m}$  Co vs.  $13.7 \pm 0.2 \mu\text{m}$  Ex,  $p < 0.05$ ) and corresponding hyperphosphorylation of protein kinase B (Akt). Absence of pathological remodelling was revealed by unchanged pro-fibrotic and pro-apoptotic markers. We found increased maximal force development ( $12.1 \pm 1.0 \text{ kN/m}^2$  Co vs.  $16.7 \pm 1.1 \text{ kN/m}^2$  Ex,  $p < 0.05$ ) and improved calcium sensitivity in the cardiomyocytes of exercised animals. Sarcomere protein investigations revealed marked overall and site-specific (Ser22/23, Ser43 and Thr143) hypophosphorylation of troponinI. We found prolonged QT interval (repolarization) and RV effective refractor period along with decreased gene expression of potassium channels. We could not induce any ventricular arrhythmia by programmed stimulation. **Conclusions:** Regular swim training induced physiological RV hypertrophy that was associated with functional improvement related to unique hypophosphorylation pattern of troponin I. A balanced exercise program without excessive exercise sessions might not be associated with induction of pathological alterations.

\* Corresponding author at: Heart and Vascular Center, Semmelweis University, Városmajor street 68, H-1122 Budapest, Hungary.

E-mail address: [o.attilio@gmail.com](mailto:o.attilio@gmail.com) (A. Oláh).

<sup>1</sup> Permanent address.

<https://doi.org/10.1016/j.yjmcc.2025.08.008>

Received 27 March 2025; Received in revised form 14 August 2025; Accepted 18 August 2025

Available online 19 August 2025

0022-2828/© 2025 The Authors. Published by Elsevier Ltd. This is an open access article under the CC BY license (<http://creativecommons.org/licenses/by/4.0/>).

## 1. Introduction

Regular exercise is associated with unequivocal health benefits and results in many structural and functional changes of the myocardium that enhance performance and prevent cardiovascular diseases [1,2]. The detailed characterization of exercise induced cardiovascular alterations have already been started more than a century ago and for a long time athlete's heart had been described as a purely benign phenomena [3,4]. Similar to left ventricle, right ventricle (RV) is also associated with increased internal diameter and free-wall thickness in highly trained athletes and the amount of heart remodelling has been traditionally considered balanced between the left and the right heart chambers [5,6]. However, in contrast to the LV, the functional consequences of RV hypertrophy have remained controversial [5,7]. Although resting RV global systolic function has shown to be decreased in endurance athletes, the novel non-invasive imaging techniques suggest unaltered or even enhanced systolic performance [8].

On the other hand, the unexplained sudden cardiac death cases and recent research findings about excessive exercise raised a question about the physiological nature of intense exercise related to elite sport [9]. Accordingly, the number of research projects about exercise-induced right ventricular alterations have extensively been increased, looking for pathophysiological characteristics [10,11]. Indeed, right ventricular wall stress is disproportionate during exercise due to the relatively thin wall of the RV and a substantial increase of pulmonary pressure during physical exertion [12,13]. As a consequence, intense prolonged exercise bouts are associated with a transient measurable reduction in right ventricular function, even when left side of the heart is relatively unaffected [14]. Chronic high-intensity exercise can not only aggravate structural diseases, such as arrhythmogenic right ventricular cardiomyopathy (ARVC), but itself might cause a pathological remodelling associated with dilation and fibrosis, a possible pro-arrhythmic remodelling [15–17].

The purpose of our study is to investigate the extent and nature of exercise-induced alterations in the RV in a small animal model, where a marked left ventricular hypertrophy was induced by regular long-lasting swim training [18]. Our animal model corresponds to relevant exercise-induced cardiac remodelling model with robust LV hypertrophy and contractility improvement. We aimed to characterize both the beneficial and potentially harmful changes in RV structure and function that result from sustained physical activity. Therefore a detailed, comprehensive characterization of regular exercise training-induced right ventricular alterations has been provided in a rat model of exercise-induced cardiac remodelling.

## 2. Materials and methods

### 2.1. Ethical approval, animals

All animals received humane care in compliance with the Principles of Laboratory Animal Care formulated by the National Society for Medical Research and the Guide for the Care and Use of Laboratory Animals prepared by the Institute of Laboratory Animal Resources and published by the National Institutes of Health (NIH Publication No. 86–23, revised 1996). Our research conform to Directive 2010/63/EU. All procedures and handling of the animals during the study were reviewed and approved by the Ethical Committee of Hungary for Animal Experimentation.

Young adult (12 wk. old,  $m = 250\text{--}300$  g) Wistar rats ( $n = 12$  male and  $n = 12$  female) (Toxi-Coop, Dunakeszi, Hungary) were housed in a room with constant temperature of  $22 \pm 2$  °C with a 12/12 h light-dark cycle and fed a standard laboratory rat diet ad libitum and free access to water.

### 2.2. Experimental groups

After acclimation, rats of the exercise group (Ex,  $n = 12$ , males and females in equal numbers) underwent a 12-week swim training program, untrained animals served as controls (Co,  $n = 12$  males and females in equal numbers). Body weight was measured three times a week during the whole study period. Invasive electrophysiological experiments were performed after completion of the training program in six exercised and six control animals (in equal proportions of the sexes) and after the protocol hearts were removed and heart weight was measured immediately after sacrifice. Six exercised and six control animals (in equal proportions of the sexes) of each groups were sacrificed without in vivo experiments, their myocardial samples were used for molecular analysis. Heart was removed under anesthesia.

### 2.3. Swim training protocol - rat model of exercise-induced cardiac hypertrophy

Based on the results of own preliminary pilot studies we provided a training plan to establish a rat model for inducing robust cardiac hypertrophy [18,19]. In brief, exercised rats swam for a total period of 12 weeks, 200 min session/day and 5 days a week. For adequate adaptation, the duration of swim training was limited to 15 min on the first day and increased by 15 min every second training session until the maximal swim duration (200 min) was reached. Untrained control rats were placed into the water for 5 min each day during the 12-week training program.

### 2.4. In vivo right ventricular electrophysiology

The procedure was performed under general anesthesia with 2 %-isoflurane in six control and six exercised animals. Body temperature was strictly maintained between 36.7 °C and 37.3 °C. An incision was made in the right supraclavicular region, and a 1.6F octapolar electrode catheter (Millar EPR-802; Millar Instruments, Houston, US) was placed in the right internal jugular vein. The catheter was advanced through the right atrium to the right ventricle using electrogram guidance and pacing capture to verify intracardiac position. A computer-based data acquisition system (PowerLab 16/30; ADInstruments, Colorado Spring, US) was used to record a 1-lead body surface ECG (lead II) and up to 4 intracardiac bipolar electrograms (LabChart Pro software v7; AD Instruments). Bipolar pacing through the distal electrodes was carried out with an impulse generator (STG3008-FA, Multi Channel Systems, Reutlingen, Germany) triggered by a special software (MC Stimulus II, Multi Channel Systems). Pacing capture intensity threshold was explored and double value of threshold intensity were used during pacing protocols.

In order to determine right ventricular refractory period (RVERP) the measurements were continued after 10 min stationary period, paying special attention to the body temperature. RVERP was tested through programmed right-atrial stimulation with a 10-beat train (S1, CL 150 ms) followed by an extrastimulus (S2) that was decreased 2 ms per step until refractoriness. Atrial effective refractory period was defined as the longest coupling interval failing to produce a propagated ventricular response.

Ventricular arrhythmia inducibility was tested with double extrastimulation (DES) and burst pacing. DES was performed following a 10-beat atrial-pacing train at a CL of 150 ms, followed by one extrastimulus (S2) 10 ms longer than RAERP, while third extrastimulus (S3) was decreased by 2 ms until refractoriness was reached. Ventricular burst pacing trains at 60 and 40 ms CL were applied for 15 and 30 s. Ventricular tachycardia (VT) was defined by  $>3$  ventricular beats. VT was considered non-sustained (nsVT) when it lasted between 1 and 30 s.

## 2.5. *In vitro* isometric force measurements in permeabilized cardiomyocytes

Deep-frozen RV tissue samples were mechanically disrupted in isolating solution (ISO, (1 mM MgCl<sub>2</sub>, 100 mM KCl, 2 mM EGTA, 4 mM ATP, 10 mM imidazole; pH 7.0, 0.5 mM phenylmethylsulfonyl fluoride, 40 μM leupeptin and 10 μM E-64, all from Sigma-Aldrich, St. Louis, MO, USA) and thereafter permeabilization was performed with 0.5 % Triton X-100 detergent for 5 min, as described elsewhere [20]. Briefly, single permeabilized cardiomyocytes were mounted with silicone adhesive (DAP 100 % all-purpose silicone sealant; Baltimore, MD, USA) to two stainless steel insect needles, which were connected to a sensitive force transducer (SensoNor, Horten, Norway) and to an electromagnetic high-speed length controller (Aurora Scientific Inc., Aurora, Canada) in ISO at 15 °C. The average sarcomere length was adjusted to 2.3 μm. The contractile machinery was activated by transferring the cardiomyocyte from a relaxing to an activating solution. The Ca<sup>2+</sup> concentrations ([Ca<sup>2+</sup>]) expressed in pCa units refer to -log [Ca<sup>2+</sup>]. The pCa of the activating and relaxing solutions was 4.75 and 9.0, respectively. When a steady force level had been reached, a rapid release-restretch maneuver (30 ms) was applied to determine the baseline of the force generation and hence the Ca<sup>2+</sup>-activated total force (F<sub>total</sub>). Fitting of the force re-development phase to a single exponential following the release-restretch maneuver allowed the characterization of the maximal turnover rate of actin-myosin cross-bridges (rate constant of force redevelopment in the presence of saturating [Ca<sup>2+</sup>]). About 6 s after the onset of force redevelopment, the Ca<sup>2+</sup>-independent passive tension (F<sub>passive</sub>) was measured by shortening to 80 % of the original preparation length at pCa 9.0 for 8 s. The active force (F<sub>active</sub>) was calculated as a difference of the F<sub>total</sub> and F<sub>passive</sub>. Maximal activation at pCa 4.75 was used to determine the maximal Ca<sup>2+</sup>-activated isometric force (F<sub>max</sub>), while activations with intermediate [Ca<sup>2+</sup>] (pCa 5.4–7.0) yielded the pCa–isometric force relationship. Isometric forces at submaximal [Ca<sup>2+</sup>] normalized to F<sub>max</sub> were plotted and then fitted to a modified Hill-equation (Origin 6.0, Microcal Software, Northampton, MA, USA) and to determine the Ca<sup>2+</sup>-sensitivity of force production (pCa50). Original forces of every individual cell were normalized to cardiomyocyte cross sectional-area, calculated from the width and height of the cardiomyocytes. Force values were expressed in kN/m<sup>2</sup> units.

## 2.6. Quantitative real-time polymerase chain reaction

Right ventricular tissue samples were homogenized in Buffer RLT (Qiagen, Venlo, The Netherlands) using Bertin Precellys 24 Tissue Homogenizer with Bertin Cryolys cooling system (Bertin Technologies, Montigny-le-Bretonneux, France) to ensure adequate and constant cooling (~0 °C) of samples throughout the procedure. Then, total RNA was isolated using the RNeasy Fibrous Tissue Kit (Qiagen) as per the manufacturer's protocol. RNA concentration was measured photometrically at 260 nm, while RNA purity was ensured by obtaining 260/280 nm and 260/230 nm optical density ratio of ~ 2.0, respectively.

Reverse transcription of RNA to cDNA was conducted with QuantiTect Reverse Transcription Kit (Qiagen) by using 1 μg RNA of each sample and random primers, as per protocol. Then, quantitative real-time polymerase chain reaction (qRT-PCR) was performed on StepOnePlus RT PCR System (Thermo Fisher Scientific, Waltham, MA, USA) using TaqMan Universal PCR MasterMix and TaqMan Gene Expression Assays (Thermo Fisher Scientific) for the following targets: α-MHC (assay ID: Rn00691721\_g1); β-MHC (assay ID: Rn00568328\_m1); atrial natriuretic factor (ANF, assay ID: Rn00561661\_m1); Bcl-2 associated X protein (Bax, assay ID: Rn02532082\_g1); Bcl-2 (assay ID: Rn99999125\_m1); connexin (Cx) 40 (Gja5, assay ID: Rn00570632\_m1); Cx43 (Gja1, assay ID: Rn01433957\_m1); potassium channels: Kcna5, assay ID: Rn00564245\_s1; Kcnd2, assay ID: Rn00581941\_m1; Kcnd3, assay ID: Rn04339183\_m1; Kcnj2, assay ID: Rn00568808\_s1; Kcnj3, assay ID: Rn00434617\_m1; matrix-metalloproteinase (MMP)-2, assay

ID: Rn01538170\_m1; MMP-9, assay ID: Rn00579162\_m1; tissue inhibitor of metalloproteinase (TIMP)-1, assay ID: Rn00587558\_m1; TIMP-2: Rn00573232\_m1 and transforming growth factor β1 (TGFβ, assay ID: Rn00572010\_m1). Every sample was quantified in duplicates or triplicates in a volume of 10 μl in each well containing 1 μl cDNA. Data were normalized to the housekeeping GAPDH, then to a positive calibrator (a pool of cDNA from all samples of the Co group) in each case. Accordingly, gene expression levels were calculated using the comparative method (2<sup>-ΔΔCT</sup>).

## 2.7. Protein expression - Western blot

Western blot experiments were performed as described earlier [19]. Snap-frozen RV samples from 6 animals of each group were homogenized with RIPA buffer (Sigma Aldrich, Budapest, Hungary) containing Complete Protease Inhibitor Cocktail (Roche, Basel, Switzerland). Protein concentration was measured by Pierce BCA Protein Assay Kit (Thermo Fisher Scientific, Rockford, IL, USA). Protein concentration was assessed with BCA kit (Thermo Fisher Scientific). Protein samples were resolved on precast 4–20 % Criterion TGX gels (Bio-Rad, Hercules, CA, USA) and transferred to Immun-Blot PVDF membranes (Bio-Rad). Equal protein loading was verified with Ponceau staining. Membranes were blocked with bovine serum albumin (BSA; Santa Cruz Biotechnology, Dallas, TX, USA) in Tris-buffered saline with 0.05 % Tween 20 (TBS-T) for 2 h. Membranes were incubated with primary antibodies in BSA in TBS-T against phospho-Akt [Ser473] (p-Akt, #4060, Cell Signaling), Akt (#9272, Cell Signaling), connective tissue growth factor (CTGF, sc-14,939, Santa Cruz) and connexin-43 (ab11370, Abcam). After three washes with TBS-T, horseradish peroxidase-conjugated secondary antibody was added for 1 h at room temperature (in BSA in TBS-T; Cell Signaling). Signals were detected with an enhanced chemiluminescence kit (Bio-Rad) by Chemidoc XRS+ (Bio-Rad) and quantitated in Image Lab 4.1 software (Bio-Rad). Antibodies bound to phospho-epitopes were removed with Pierce Stripping Buffer (Thermo Fisher Scientific) before incubation with antibodies detecting the total protein. We included all intact samples in the analysis.

The sarcomeric proteins were detected as follows: Cardiomyocytes were solubilized in sample buffer (containing 8 M urea, 2 M thiourea, 3 % (w/v) sodium dodecyl sulfate (SDS), 75 mM DTT, 50 mM Tris-HCl, pH 6.8, 10 % (v/v) glycerol, bromophenol blue, 40 μM leupeptin and 10 μM E-64, Sigma-Aldrich, St. Louis, MO, USA) followed by 45 min vortexing. After centrifugation (16,000 g for 5 min at 24 °C), protein amount of the supernatant was determined by the dot-blot technique using bovine serum albumin (BSA, Sigma-Aldrich, St. Louis, MO, USA) standard, and the concentration of the samples was set to 2 mg/ml. Agarose-strengthened 2 % SDS-polyacrylamide gels were used to separate N2B titin. Total phosphorylation status of titin protein was assessed by Pro-Q® Diamond phosphoprotein staining (Invitrogen, Eugene, OR, USA) according to the manufacturer's protocol, while total amount of protein was stained by Coomassie blue (Reanal, Budapest, Hungary). Western immunoblotting was applied to assess site-specific phosphorylation status of cTnI. Separation of cTnI and cMyBP-C was carried out in 4 % and 12 % polyacrylamide gels, respectively. After PAGE and protein blotting procedure, the membranes were blocked with 2 % BSA diluted in PBS containing 0.1 % (v/v) Tween 20 (PBST, Sigma-Aldrich, St. Louis, MO, USA) for 30 min, then cTnI phosphorylation-sensitive antibodies were used to determine the levels of PKA- and PKC-dependent cTnI (Ser-23/24 (1:1000), Ser-43 (1:500) and Thr-143 (1:500), Abcam, Cambridge, UK) phosphorylation. The signal was detected with a peroxidase-conjugated anti-rabbit IgG secondary antibody (1:300) (Sigma-Aldrich, St. Louis, MO, USA) in nitrocellulose membranes. Total protein amounts were visualized with super sensitive membrane staining (UD-GenoMed, Debrecen, Hungary). Chemiluminescence (ECL) signals of site-specific phosphorylation of cTnI and cMyBP-C were normalized to a Western immunoblot stain.

## 2.8. Histology

A whole transversal section of myocardium were cut at the height of base and left ventricular papillary muscles. Ventricular myocardial tissue samples of animals were removed for histological processing and then they were fixed in neutral buffered formalin (4 %) and embedded in paraffin. Slices of the whole heart at the level of LV papillary muscles were sectioned and processed conventionally for histological examination.

After staining these myocardial tissue sections with hematoxylin and eosin (H&E) the tissue structure was examined by light microscopy. The transverse, transnuclear diameter of 100 randomly selected RV cardiomyocytes per animal in longitudinal orientation of HE stained sections were measured using the ImageJ software (National Institutes of Health, Bethesda, MD, USA), and then averaged per animal.

To assess cardiomyocyte cross-sectional area (CSA), we performed laminin antibody-based histochemistry approach using frozen-fixed histological slices (12  $\mu\text{m}$ ) of RV. The slides were warmed at room temperature for 30 min. After pre-warming for 30 min, the samples were fixed in ice-cold acetone for 5 min and air-dried for 30 min. Following three 5-min washes with  $1 \times$  PBS, non-specific binding sites were blocked with 2.5 % serum (corresponding to the secondary antibody) and 2.5 % milk for 1 h. The primary antibody (anti-laminin, Sigma-Aldrich, L9393, 1:50) was incubated overnight at 4 °C. Subsequently, incubation with secondary antibodies, such as AlexaFluor 568 anti-rabbit antibody, was conducted for 1 h at room temperature. Finally, the nuclei were stained with DAPI (diluted 1:5000 in PBS) for 5 min. CSA values (approximately 1000 per animal) were measured by ImageJ software after taking snapshots by a Leica LMD6 microscope.

RV wall thickness was measured on scanned H&E slices at the height of LV papillary muscles. RV free wall thickness was measured three times (ImageJ software), perpendicularly to RV endocardial surface and these values were averaged.

To investigate RV collagen content, picosirius red positive area was calculated using ImageJ image analysis software. Three randomly selected RV fields (magnification  $200\times$ ) were investigated from each animal. The fractional area (picrosirius red positive area to total area ratio) was determined on each images and the mean value of the images represents each animal.

Apoptosis in cardiomyocytes was determined with terminal deoxynucleotidyl transferase-mediated dUTP nick-end labeling (TUNEL) technique. TUNEL staining was performed using DeadEnd™ Colorimetric TUNEL System (Promega, Madison, WI, USA) according to the manufacturers instruction. Three visual fields of right ventricular sections were randomly selected in each animal, and TUNEL-positive cells were counted.

## 2.9. Proteomic analysis

8 exercised and 8 control animals (males and females equally) were included in proteomic analysis. Cryopreserved LV and RV myocardial samples were homogenized in 0.1 % Rapigest and 100 mM HEPES (pH 7.5) solution. Reductive alkylation was performed using 5 mM tris(2-carboxyethyl)phosphine-hydrochloride (TCEP, Sigma-Aldrich) and 20 mM iodoacetamide (Sigma-Aldrich). Proteins were digested overnight by Trypsin (Worthington, Lakewood, NJ, sequencing grade), and the resulting peptides were desalted on PreOmics columns (PreOmics, Bavaria, Germany). Further steps were performed as described previously. Briefly, peptides were labeled with TMT16plex isobaric label reagents (Thermo Fisher Scientific). Reverse-phase pre-fractionation (pH = 10) was performed on an XBridge C18 column, 150 mm  $\times$  1 mm column containing 3.5  $\mu\text{m}$  particles (Waters) inserted into an Agilent 1100 high performance liquid chromatography system (HPLC). Fractions were analyzed on a Q-Exactive Plus (Thermo Scientific, Bremen, Germany) operating in a data-dependent acquisition (DDA) mode. Mass spectra were analyzed using MaxQuant version 1.6.17.0 with the

Uniprot rat database downloaded in November 2020. For dimension reduction of the proteomic dataset, partial least squares – discriminant analysis (PLS-DA) was performed using the mixOmics R package. Quantified peptide intensities were then summarized by MSstatsTMT (R package). Proteomic data were uploaded to MassIVE system (identification number: MassIVE MSV000098270).

## 2.10. Statistics

Graphs were created and statistical analysis was performed in GraphPad Prism 6.0 software. Differences between groups were calculated by Student's test after confirmation of normal distribution of the parameters. Group descriptions were based on the mean  $\pm$  SEM values. Statistical significance was accepted at  $p < 0.05$ .

## 3. Results

### 3.1. Right ventricular hypertrophy

Exercise training was associated with significant, marked myocardial hypertrophy, indexed by the heart weight values normalized to body weight (Fig. 1.A). We observed RV hypertrophy in trained animals at the macroscopic and microscopic levels. RV free wall was mildly thickened in exercised rats compared to control ones. Accordingly, RV cardiomyocyte width was also increased after the completion of swim training protocol (Fig. 1.A). Laminin-stained RV myocardial sections also suggested approximately 15 % hypertrophy of RV cells. The phosphorylation level of protein kinase B (Akt), a key regulator of physiological hypertrophy, was also increased in exercised rodents, while the total Akt level did not differ between groups (Suppl. Material).

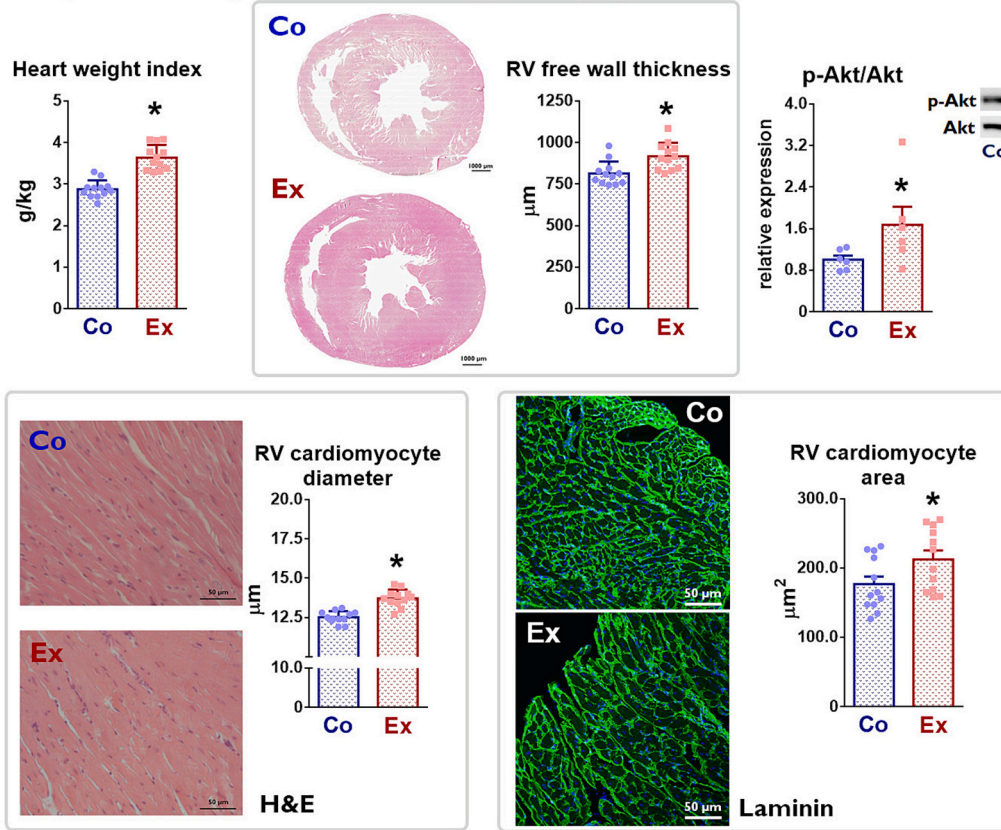
We investigated the nature of the observed RV hypertrophy. Therefore, gene expression level of common markers of pathological hypertrophy were measured. Neither ANF, nor the ratio of  $\alpha$ - and  $\beta$ -MHC did differ between exercised and control animals (Fig. 1.B). Moreover, TUNEL staining did not suggest any apoptotic activity of the cells (lack of stained cell nuclei) and the gene expression ratio between proapoptotic Bax and anti-apoptotic Bcl-2 remained unchanged after exercise training. These results suggest physiological nature of the observed RV hypertrophy. The histological analysis of picosirius-stained RV sections allowed us to estimate the collagen content of the myocardium and according to our results, exercise training was not related to myocardial fibrosis (Fig. 1.C). Accordingly, the gene expression level of TGF- $\beta$ 1 and the protein expression of CTGF did not reveal the induction of profibrotic processes. MMP/TIMP ratios were even decreased, because of the increased gene expression of TIMPs, without alteration in expression of MMPs.

Proteomic analysis suggested less pronounced exercise-induced alterations in the RV compared to the changes in LV (Fig. 2A.). In contrast to LV data, there was a moderate overlap in the RV proteomic pattern (shown by partial least squares-discriminant analysis, Fig. 2A) of control and exercised animals. While we detected 293 altered proteins in the LV, this number was only 38 in case of the RV (Figure 2B). Our proteomic method could not identify the presence of distinct clusters or pathway by gene ontology or pathway analysis, we could identify specific proteins that showed characteristic alterations in the RV. We listed the proteins (by their genes name) with considerable alterations in the RV on Fig. 2C. Although a few proteins showed isolated change, most of them was also associated with similar alterations in the left ventricle (Fig. 2C).

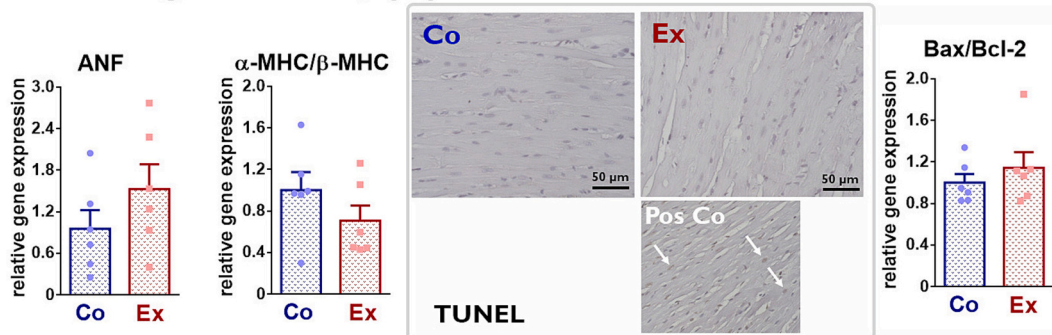
### 3.2. Myocardial sarcomerodynamics and phosphorylation pattern of myofilaments

Ca<sup>2+</sup>-activated force ( $F_{\text{active}}$ ) development was followed in permeabilized cardiomyocytes isolated from RV tissue samples in vitro at different Ca<sup>2+</sup> concentrations (pCa: from 4.75 to 7.0) (Fig. 3A). Mean

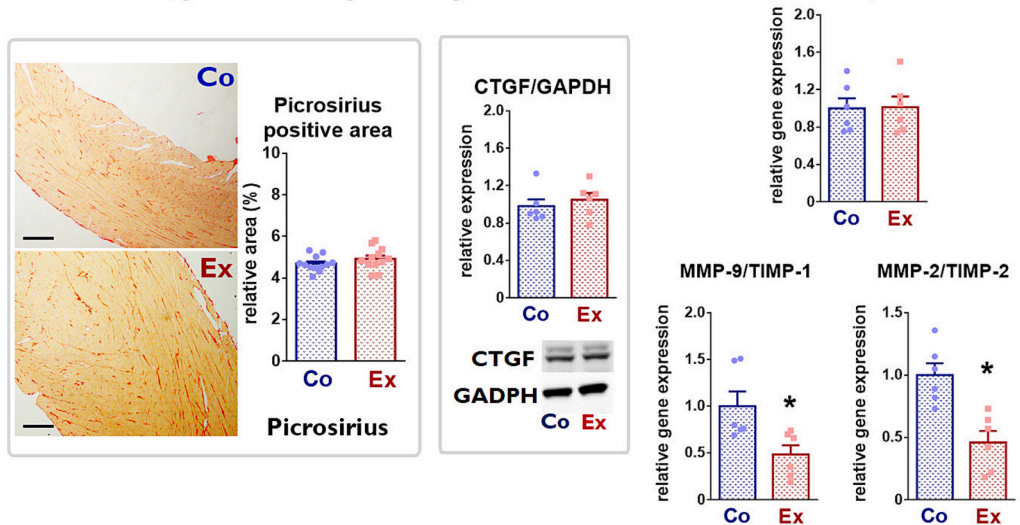
### A Myocardial/right ventricular hypertrophy



### B Pathological markers, apoptosis



### C Fibrosis, profibrotic pathways



(caption on next page)

**Fig. 1.** Exercise-induced tissue remodelling in the right ventricle (RV). Panel A: markers of myocardial and RV hypertrophy: heart weight index (normalized to body weight), RV free wall thickness and RV cardiomyocyte diameter (H&E) and area (laminin) suggested RV hypertrophy in exercised (Ex) animals compared to control (Co) ones ( $n = 12/\text{group}$ ). This was associated with hyperphosphorylation of protein kinase B (Akt) ( $n = 6/\text{group}$ ). Panel B: markers of pathological remodelling (ANF, ratio of  $\alpha$ -MHC and  $\beta$ -MHC) and apoptosis (TUNEL positive nuclei, Bax/Bcl-2 gene expression ratio) did not differ between groups ( $n = 6/\text{group}$ ). Panel C: markers of fibrotic processes (collagen content by Picrosirius, TGF-  $\beta$ 1, CTGF) and MMP/TIMP ratios were even decreased in exercised animals ( $n = 6/\text{group}$ ). Akt: protein kinase B; ANF: atrial natriuretic factor; Bax: Bcl-2 associated protein X; Co: control group, CTGF: connective tissue growth factor; Ex: exercised group, GAPDH: Glyceraldehyde-3-phosphate dehydrogenase; H&E: hematoxylin-eosin, MHC: myosin heavy chain; MMP: matrix metalloproteinase; Pos Co: positive control of TUNEL staining; TIMP: Tissue inhibitor of metalloproteinase; TUNEL: terminal deoxynucleotidyl transferase dUTP nick end labelling. Scale bar on picrosirius staining: 100  $\mu\text{m}$ . Data: mean  $\pm$  SEM. \* $p < 0.05$  vs. Co. Student's  $t$ -test was used.

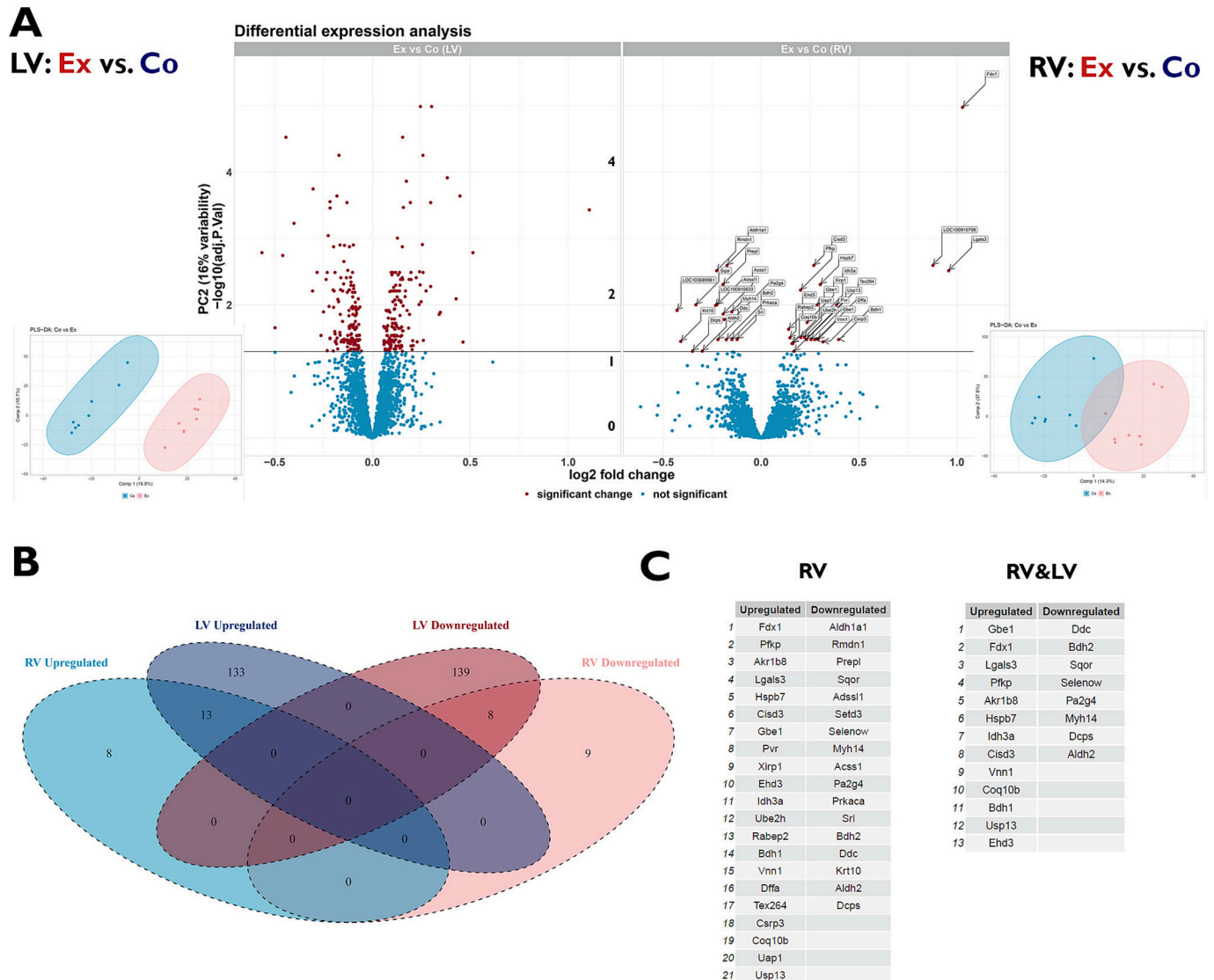


**Fig. 2.** Proteomic analysis. Panel A: Volcano-plot about the proteomic alterations in the left ventricle (LV) and the right ventricle (RV), when the proteomic expression of exercised (Ex) animals was related to control (Co) ones ( $n = 8/\text{group}$ ). Significantly altered proteins has been shown as red dots, while unchanged proteins are marked with blue dots. Partial least squares – discriminant analysis (PLS-DA) in the RV showed a considerable overlap, while there was marked separation in the LV. Panel B: The numbers of significantly changed proteins in case of the LV and RV. Note, that while proteomic analysis revealed 293 altered proteins in LV, this number was only 38 in case of RV. Panel C: we listed the significantly altered proteins in the RV and also highlighted those showed similar alterations in the LV and RV. (For interpretation of the references to colour in this figure legend, the reader is referred to the web version of this article.)

values of  $F_{\text{active}}$  (incl.  $F_{\text{max}}$ ) were significantly higher following exercise training (Ex group) than those of controls (Co group) between pCa 6.2 and 4.75.  $\text{Ca}^{2+}$ -sensitivity of force production (pCa50) was significantly higher in the Ex group than in the Co group. Mean pCa50 values did not differ after detraining (Fig. 3B). Passive tension ( $F_{\text{passive}}$ ) of cardiomyocytes and the the rate of tension development ( $k_{\text{tr,max}}$ ) were similar in the Co and Ex groups.

Following exercise training, overall phosphorylation level of cTnI

decreased markedly in RV cardiomyocytes. Overall phosphorylation levels of cMyBP-C and titin were similar in permeabilized RV cardiomyocytes in both experimental groups (Fig. 4A). To elucidate the molecular background of increased  $F_{\text{max}}$  and pCa50 values of exercised animals, site-specific phosphorylation assays were included for cTnI. Hypophosphorylation both at the PKA-specific Ser22/23 and at the PKC-specific Ser43 and Thr143 sites of cTnI were observed in the Ex groups (Fig. 4B). These sites might be associated with the observed improved

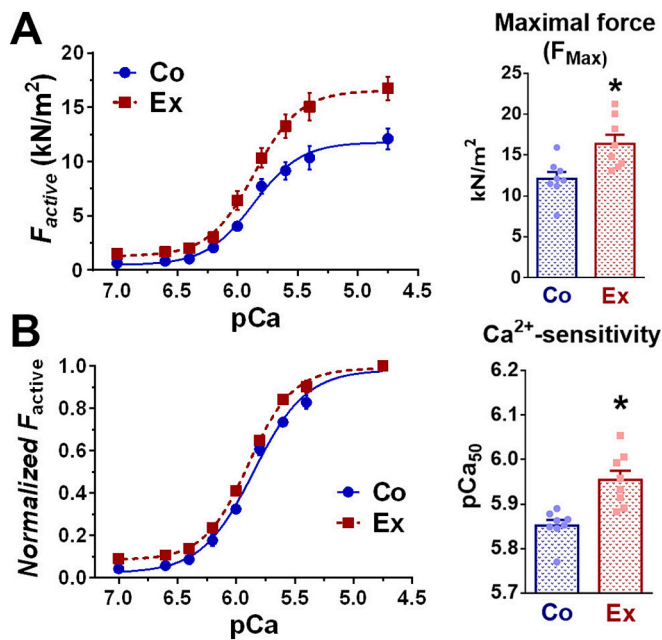


**Fig. 3.** Sarcomerodynamics in isolated cardiomyocytes of right ventricle (RV). Panel A: Calcium concentration (pCa)-developed force ( $F_{active}$ ) relationships from one-one animal of each group (between pCa 7 and 4.75). The maximal  $Ca^{2+}$ -activated force ( $F_{max}$ ) was improved in the RV cardiomyocytes of exercised (Ex) animals compared to control (Co) ones. Panel B: normalized pCa-force relationships from one-one animal of each group (between pCa 7.0 and 4.75). The leftward shift of the curve and consecutive increased pCa<sub>50</sub> values in exercised animals revealed improved  $Ca^{2+}$ -sensitivity induced by exercise training ( $n = 8$ /group).

Co: control group, Ex: exercised group. Data: mean  $\pm$  SEM. \* $p < 0.05$  vs. Co. Student's *t*-test was used.

contractility in exercised animals.

### 3.3. Electrophysiological alterations

We performed *in vivo* invasive electrophysiology to obtain electrical properties of the RV myocardium. Refractoriness of RV myocardium was measured by standard protocol and we found a significant prolongation of RVERP in exercised rats (Fig. 5A). Right ventricular arrhythmia inducibility was tested by burst pacing and DES stimulation protocols (Fig. 5B). No sustained ventricular arrhythmia was triggered by these programmed stimulations. We could detect one induced VES in the case of one control and one exercised animal (Fig. 5C). These data suggest that our training protocol did not result in increased risk of arrhythmia in exercised animals. We found decreased RV gene expression of potassium channels (Kcnd2, Kcnd3 and Kcnj3) in exercised animals compared to controls. The gene and protein expression of connexins did not differ between groups (Fig. 5D).

## 4. Discussion

The knowledge of exercise-induced cardiovascular alterations have been substantially widened in the recent years. However, the role of right ventricle in cardiovascular adverse events observed in elite athletes is still dubious. According to our knowledge, this is the first comprehensive experimental study to characterize long-lasting, intense training associated right ventricular alterations. We investigated different aspects of right ventricular remodelling in a rat model, where relevant, significant hypertrophy and contractility improvement was described in the left ventricle [18,21].

### 4.1. Right ventricular remodelling

Indeed, 12-week long swim training program has induced ~20–25% myocardial hypertrophy in our exercised animals compared to the control ones, that is comparable to highly-trained athletes, other relevant animal models and our previous results [19,22,23] (Fig. 1A). We also detected hypertrophy of the right ventricular cardiomyocytes and increased RV free wall thickness and area values (unloaded conditions), that should be the consequence of increased pulmonary pressure and the general volume overload during swim training sessions. Accordingly, endurance elite and master athletes were both characterized by significantly increased RV mass in MRI studies, where usually sport was associated RV hypertrophy and dilation [24,25]. We also detected increased protein kinase B (Akt) phosphorylation in RV cardiomyocytes that suggest the activation of the main pathway that is associated with physiological hypertrophy (Fig. 1A, 26).

To further confirm the physiological nature of the detected hypertrophy, we examined markers of pathological remodelling at the cellular level and in the myocardium. These markers can clearly differentiate between physiological and pathological myocardial processes [26,27]. We could not detect any induction of genes as ANF or the ratio of MHC isoforms (Fig. 1B). Myocardial pathological processes and excessive oxidative stress might lead to increased number of programmed cell death in the myocardium [26,27]. Neither TUNEL staining, nor the ratio of pro-apoptotic Bax and anti-apoptotic Bcl-2 have suggested increased apoptotic activity in the RV of trained animals (Fig. 1B).

Perhaps, the most dubious question about exercise-induced RV alterations is about the long-term remodelling and fibrosis that was raised mostly by the persistence of RV dilation in veteran athletes. Human cardiac MRI studies have found delayed gadolinium enhancement (focal pattern, especially at the interventricular septum and the site of RV attachment) in approximately 10–40% of active and veteran endurance athletes [10,28,29]. Theoretically the effect of disproportionate hemodynamic loading during exercise session might lead to long-term pathological consequences [13]. Besides that, there are several small animal studies, where a marked right ventricular fibrosis and induction of profibrotic processes were observed after intense, vigorous exercise training program [17,30,31]. Not only the type of intensity and length of training might affect the pathological or physiological phenotype of hypertrophy, but the role of stress should be thoroughly investigated in animal models. Our data indicated lack of fibrosis in swim-trained rats, despite the significant hypertrophy (Fig. 1B). We could not detect the induction of profibrotic key regulator molecules (such as TGF- $\beta$ 1 and CTGF), that is in line with our histological analysis. We detected even decreased expression ratio of the most abundant MMPs and TIMPs in the RV myocardium of exercised rats. The increased TIMP expression without alteration of MMP expression suggests rather antifibrotic processes in the exercised myocardium. There are also several human studies that are in line with our findings and show absence of myocardial fibrosis [32,33]. The results of our study suggest that long-term balanced exercise alone may not induce RV fibrotic processes. Indeed, there are considerations about the pathological precipitating role of recurrent excessive exercise sessions (such as races) and related extreme pulmonary hypertension [16].

Proteomic analysis revealed characteristic differences between LV and RV that suggests different molecular response to exercise training. Interestingly, the disproportionately increased load of RV led to milder molecular alterations. In case of the RV, only a few proteins showed upregulation and downregulation (Fig. 2A. and B.). While we could not identify any characteristic pathway or ontological cluster change, a few proteins could be recognized to be involved in both exercise-induced LV and RV remodelling (Fig. 2C.). Most of them plays role in mitochondrial biogenesis or is associated with cardioprotection: galectin-3 (Lgals3, protective effect by reducing the level of inflammation and apoptosis) [34], ferredoxin-1 (Fdx1, biogenesis of mitochondrial cytochrome *c* oxidase) [35], Hspb7 (a cardioprotective chaperone facilitating

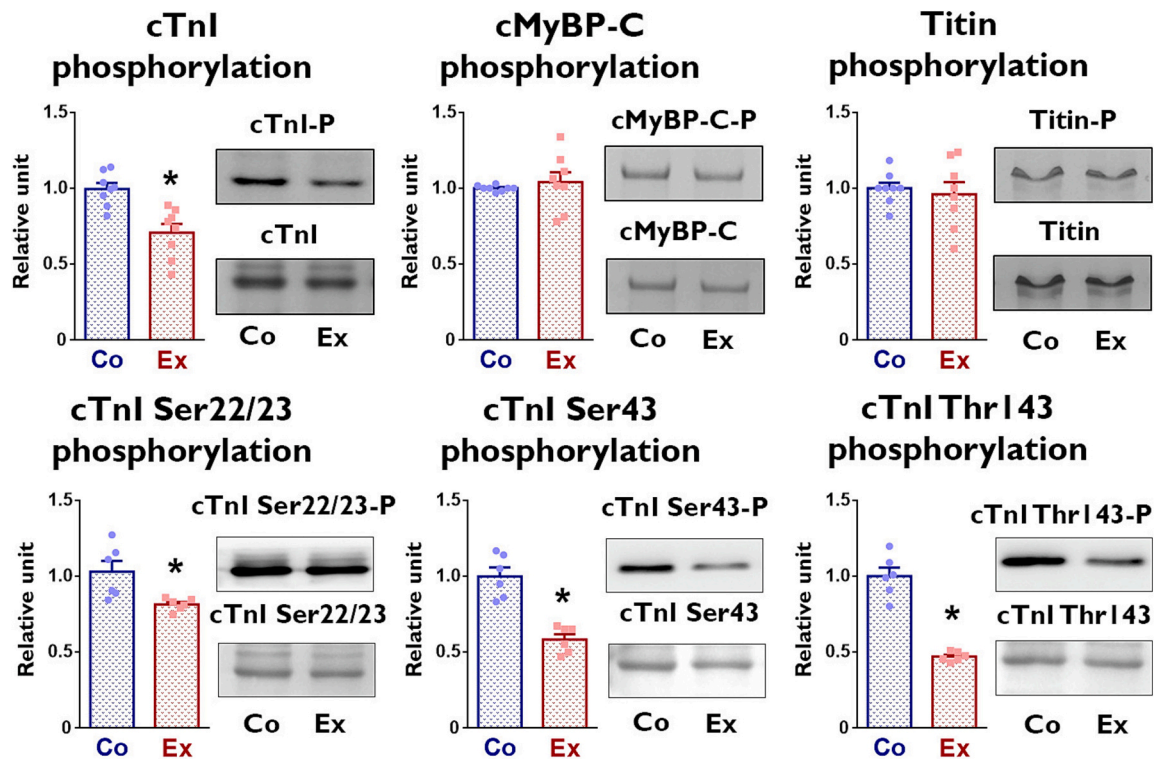


**Fig. 4.** Phosphorylation levels of sarcomeric proteins of right ventricular RV cardiomyocytes following exercise training. Upper panel: Pro-Q Diamond staining was used to detect total phosphorylation level of cardiac troponin I (cTnI), cardiac myosin binding protein-C (cMyBP-C) and titin in RV. Exercise training was associated with decreased TnI phosphorylation level, while there was no difference regarding phosphorylation of cMyBP-C and titin ( $n = 8/\text{group}$ ). Total protein amounts were assessed by Coomassie-blue staining. Lower panel: Site-specific phosphorylation levels of cTnI. cTnI phosphorylation levels of the Ser-22/23, Ser-43 and Thr-143 residues were determined by Western immunoblotting in RV cardiomyocytes ( $n = 6/\text{group}$ ). We found marked hypophosphorylation on these sites. The upper bands reflect the phosphorylation status of proteins and the lower bands indicate total protein amounts. Co: control group, Ex: exercised group. Data: mean  $\pm$  SEM. \* $p < 0.05$  vs. Co. Student's t-test was used. (For interpretation of the references to colour in this figure legend, the reader is referred to the web version of this article.)

sarcomeric proteostasis [36], Cisd3 (important for supporting the biogenesis and function of mitochondrial respiratory complex) [37], Vnn1 (Vanin-1, required for the maintenance of mitochondrial homeostasis) [38], Coq10b (mitochondrial coenzyme Q-binding protein CoQ10 homolog B) [39] and Bdh1 (key enzyme in the regulation of myocardial ketone body uptake and oxidation) [40]. Further studies are needed to explore exercise-associated molecular alterations in detail.

#### 4.2. Function: sarcomerodynamics and sarcomeric alterations

The hemodynamic load on the right ventricle is considered more pronounced during exercise than that on the left ventricle. The thin wall of RV with a disproportionately increased pulmonary pressure can cause a suboptimal coupling throughout high-intensity exercise. These alterations can lead to exercise-induced transient RV fatigue that has been widely described: not only the systolic function but also the relaxation can be impaired following prolonged exercise [41,42].

Regarding RV function, the long-term consequence of regular training remained controversial. Most of the studies showed that echocardiographic parameters of global RV systolic function (ejection fraction, fractional area change) were slightly reduced or comparable at rest compared with the non-athletic controls [43,44]. Indeed, a mild reduction in conventionally measured RV function at rest has been considered a physiological phenomenon associated with RV dilation and comparable contractile reserve was shown during exercise [5,10]. However, these parameters are largely dependent on chamber sizes and loading conditions of the RV. According to our knowledge, our experimental study is the first one to show that RV cardiomyocytes are associated with improved contractile force,  $\text{Ca}^{2+}$ -sensitivity and contractile

capacity (Fig. 3). We should also add, that the increment in maximal force ( $\sim +40\%$ ) is relatively smaller compared to LV (almost doubled) according to our previous results [20].

The mechanism in the background of improved RV contractile reserve is still unknown. While there were slight proteomic alterations, we investigated the phosphorylation pattern of myofilaments (Fig. 4). While the total phosphorylation of cMyBP-C did not show difference, we have found marked hypophosphorylation of cTnI. Indeed cTnI holds a central role in the regulation of contraction and relaxation in the heart muscle [45]. Furthermore, we investigated phosphorylation sites those are associated with alteration of contractile status and  $\text{Ca}^{2+}$ -sensitivity (Fig. 4) [46]. While Ser22/23 is dependent on protein kinase A or G, all of the investigated sites (Ser22/23, Ser43, Thr143) are regulated by protein kinase C (PKC). PKC-dependent phosphorylation of cTnI has been suggested to contribute to the reduction in maximum  $\text{Ca}^{2+}$ -activated force in failing human myocardium. Increased phosphorylation of Ser43 was related to decreased  $\text{Ca}^{2+}$ -activated force and phosphorylation of Ser22/23 was associated with decreased  $\text{Ca}^{2+}$ -sensitivity [46]. Although the interpretation of myofilament phosphorylation is complex, here we found quite similar phosphorylation pattern as in the LV that can be unique in exercise-induced hypertrophy [20]. Further studies are needed to understand the regulation of troponin I in athletes.

Moreover, in this study we found no difference regarding  $F_{\text{passive}}$  (indicating passive diastolic function) and no alteration in titin phosphorylation was observed (Figs. 3 and 4.). This is in line with the absence of fibrotic remodelling and shows similar result to our previous study about LV [20].

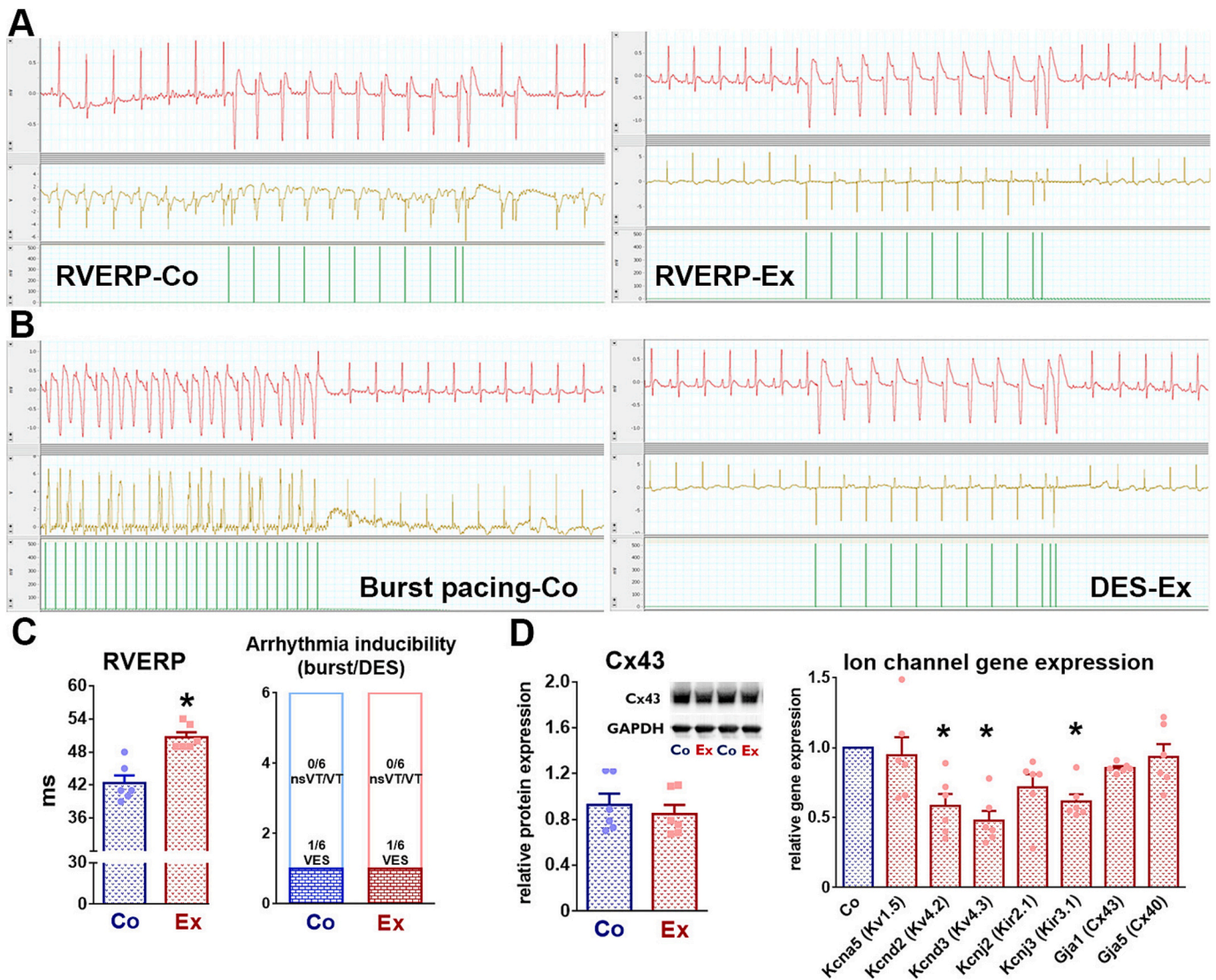


**Fig. 5.** Electrophysiological properties of the right ventricle (RV) by invasive electrophysiology and molecular measurements. Panel A: Right ventricular refractory period (RVERP) representative ECG (red), IAEG (yellow) and stimulation (green) curves from an exercised (Ex) and a control (Co) animal. Panel B: Ventricular arrhythmia inducibility by using burst pacing or double extrastimulation (DES) protocol and representative ECG (red), IAEG (yellow) and Stim curves from an exercised and a control animal. Panel C: RVERP values were increased in exercised animals. We could not induce non-sustained ventricular tachycardia (nsVT) or ventricular tachycardia (VT) in our animals, while in case of one-one animal, we could induce ventricular extrasystole (VES). Panel D: RV protein expression of connexin-43 (Cx43) did not differ between groups. RV gene expression of different voltage-gated potassium channels (Kv1.5, Kv4.2 and Kv4.3), inward rectifier potassium channels (Kir2.1 and Kir3.1) and connexins (Cx40 and Cx43) in control and exercised animals ( $n = 6$ /group for all measurements).

Co: control group, Ex: exercised group. Data: mean  $\pm$  SEM. \* $p < 0.05$  vs. Co. Student's t-test was used. (For interpretation of the references to colour in this figure legend, the reader is referred to the web version of this article.)

#### 4.3. Electrical alterations

In those minority of athletes who develop ventricular arrhythmias, the origin of arrhythmias is most likely to be in the RV and is frequently associated with more pronounced dilation [16]. Although small animal models hold considerable limitations we examined the electrical properties of RV. Exercise-induced RV hypertrophy was associated with increased refractory period (RVERP, Fig. 5A). This is in line with this alteration, where our research groups and others have found prolonged repolarization (QT length) after completion of exercise training [47,48]. This is also in accordance with a study, where longer VERP was detected on isolated heart of trained rabbits [49]. Longer refractory period, without excessive prolongation, might hold rather a protective role against re-entrant arrhythmias [50]. We could not induce ventricular arrhythmias by forceful programmed stimulation (Fig. 5B). Our finding is in contrast with previous studies that showed inducible ventricular

arrhythmia in treadmill-trained small and large animals [30,48]. However, in these investigations, the increased arrhythmia inducibility was associated with significant RV fibrotic remodelling. Our data is in line with the previously described benign nature of exercise-induced hypertrophy in a healthy myocardium and underline the beneficial effects of regular intense training [32,33,47]. Decreased RV expression of certain potassium channels was observed in the RV and similar alterations have been described in the atrium of exercised animals [47]. The decreased expression of potassium channels might lead to smaller potassium outward currents and might explain the prolonged (slower) repolarization and refractoriness of the myocardium, although the markedly distinct repolarization in rodents makes it difficult to extrapolate this result to athletes. However, this data is in line with a previous observation that suggested a reduction in density of one component of repolarizing  $K^+$ -currents [51].

## 5. Conclusions

Regular prolonged endurance training resulted in a physiological, beneficial remodelling of the right ventricle without induction of pathological processes. We have found a significant right ventricular functional improvement by increased maximal activated force and calcium sensitivity of isolated cardiomyocytes. In the background significant hypophosphorylation of troponin I was observed, quite similar pattern to left ventricle. In vivo electrophysiology has not revealed increased myocardial vulnerability towards ventricular arrhythmias. According to our results the previously observed pathological concerns about right ventricle in athletes might be the consequence of excessive exercise sessions (prolonged competitions) or other triggers (persistent hypertension) or might be based on other right ventricular pathologies.

The unexplained sudden cardiac death cases and recent pathological findings about excessive exercise raised a question about the physiological nature of intense exercise related to elite sport. Especially the role of right ventricular remodelling has been suspected in the background, because of the disproportionate load during exercise sessions and sporadic findings of right ventricular fibrosis. We investigated right ventricular alterations in our small animal model that is associated with training-induced robust cardiac hypertrophy and functional improvement. A significant right ventricular hypertrophy was observed with the absence of pathological myocardial processes. Contractile reserve and calcium sensitivity improvement was shown on right ventricular isolated cardiomyocytes. A marked hypophosphorylation of troponin I was observed, both total and contractility-associated sites were involved. In vivo electrophysiology could not show any sign of increased arrhythmia vulnerability. Our results strengthen the hypothesis that regular intense exercise does not lead to pathological right ventricular remodelling in a healthy myocardium. The previously observed sporadic cases might be the consequence of non-severe structural heart disease or might be related to excessive prolonged exercise sessions or other trigger factors.

## CRedit authorship contribution statement

**Attila Oláh:** Writing – original draft, Methodology, Investigation, Conceptualization. **Beáta Bódi:** Methodology, Investigation. **Bálint András Barta:** Methodology, Investigation. **Ólivia Bottlik:** Methodology, Investigation. **Alex Ali Sayour:** Methodology, Investigation. **Mihály Ruppert:** Methodology, Investigation. **Karolina Katarzyna Kolodziejka:** Methodology, Investigation. **Andrea Kovács:** Methodology, Investigation. **Zoltán V. Varga:** Methodology, Investigation. **Péter Ferdinandy:** Writing – review & editing, Investigation. **Oliver Schilling:** Writing – review & editing, Methodology, Investigation. **Zoltán Papp:** Writing – review & editing, Conceptualization. **Béla Merkely:** Writing – review & editing, Conceptualization. **Tamás Radovits:** Writing – review & editing, Investigation, Funding acquisition, Conceptualization.

## Ethics approval statement

All animals received humane care in compliance with the Principles of Laboratory Animal Care formulated by the National Society for Medical Research and the Guide for the Care and Use of Laboratory Animals prepared by the Institute of Laboratory Animal Resources and published by the National Institutes of Health (NIH Publication No. 86–23, revised 1996). All procedures and handling of the animals during the study were reviewed and approved by the Ethical Committee of Hungary for Animal Experimentation.

## Declaration of generative AI and AI-assisted technologies in the writing process

The authors did not use generative AI or AI-assisted technologies in the development of this manuscript.

## Funding source

This work was supported by the National Research, Development, and Innovation Office of Hungary (NKFIH; K120277 and K135076 to BM; K147173 to ZP and EKÖP-2024-12 to BAB), by the János Bolyai Research Scholarship of the Hungarian Academy of Sciences (BO/00837/21 to AO), and by the New National Excellence Program of The Ministry for Innovation and Technology (ÚNKP-21-5-SE-19 to AO).

## Declaration of competing interest

None.

## Acknowledgements

We gratefully acknowledge Eduard Guasch, who introduced us to the theoretical and practical experimental cardiac electrophysiology. We would thank to Daria Chalkova widening the interpretation of proteomic analysis. Expert technical assistance of Henriett Biró, Gábor Fritz, Benjamin Prokaj, Ádám Steiner and Edina Urbán is greatly acknowledged.

## Appendix A. Supplementary data

Supplementary data to this article can be found online at <https://doi.org/10.1016/j.yjmcc.2025.08.008>.

## References

- [1] C. Fiuzza-Luces, N. Garatachea, N.A. Berger, A. Lucia, Exercise is the real polypill, *Physiology (Bethesda)* 28 (2013) 330–358.
- [2] A. Oláh, A.A. Sayour, M. Ruppert, et al., Dynamics of exercise training and detraining induced cardiac adaptations, *Curr. Opin. Physiol.* (2023) 33.
- [3] G. Pavlik, Z. Major, B. Varga-Pintér, M. Jeserich, Z. Kneffel, The athlete's heart part I (review), *Acta Physiol. Hung.* 97 (2010) 337–353.
- [4] D.L. Prior, A. La Gerche, The athlete's heart, *Heart* 98 (2012) 947–955.
- [5] A. D'Andrea, A. La Gerche, E. Golia, et al., Physiologic and pathophysiological changes in the right heart in highly trained athletes, *Herz* 40 (2015) 369–378.
- [6] A. La Gerche, T. Roberts, G. Claessen, The response of the pulmonary circulation and right ventricle to exercise: exercise-induced right ventricular dysfunction and structural remodeling in endurance athletes (2013 Grover conference series), *Pulm. Circ.* 4 (2014) 407–416.
- [7] V. Conti, F. Migliorini, M. Piloni, et al., Right heart exercise-training-adaptation and remodelling in endurance athletes, *Sci. Rep.* 11 (2021) 22532.
- [8] B.K. Lakatos, O. Kiss, M. Tokodi, et al., Exercise-induced shift in right ventricular contraction pattern: novel marker of athlete's heart? *Am. J. Physiol. Heart Circ. Physiol.* 315 (2018) 1640–1648.
- [9] S. Sharma, A. Merghani, L. Mont, Exercise and the heart: the good, the bad, and the ugly, *Eur. Heart J.* 36 (2015) 1445–1453.
- [10] A. La Gerche, A.T. Burns, D.J. Mooney, et al., Exercise-induced right ventricular dysfunction and structural remodelling in endurance athletes, *Eur. Heart J.* 33 (2012) 998–1006.
- [11] S. Pujadas, M. Doñate, C.H. Li, et al., Myocardial remodelling and tissue characterisation by cardiovascular magnetic resonance (CMR) in endurance athletes, *BMJ Open Sport Exerc. Med.* 4 (2018) e000422.
- [12] A. La Gerche, H. Heidbüchel, A.T. Burns, et al., Disproportionate exercise load and remodeling of the athlete's right ventricle, *Med. Sci. Sports Exerc.* 43 (2011) 974–981.
- [13] R. Lakin, R. Debi, S. Yang, N. Polidovitch, J.M. Goodman, P.H. Backx, Differential negative effects of acute exhaustive swim exercise on the right ventricle are associated with disproportionate hemodynamic loading, *Am. J. Physiol. Heart Circ. Physiol.* 320 (2021) H1261–H1275.
- [14] A.D. Elliott, A. La Gerche, The right ventricle following prolonged endurance exercise: are we overlooking the more important side of the heart? A meta-analysis, *Br. J. Sports Med.* 49 (2015) 724–729.
- [15] J. Saberniak, N.E. Hasselberg, R. Borgquist, et al., Vigorous physical activity impairs myocardial function in patients with arrhythmogenic right ventricular cardiomyopathy and in mutation positive family members, *Eur. J. Heart Fail.* 16 (2014) 1337–1344.
- [16] A. La Gerche, D.J. Rakhit, G. Claessen, Exercise and the right ventricle: a potential Achilles' heel, *Cardiovasc. Res.* 113 (2017) 1499–1508.
- [17] F. Maleki, J. Mehrabani, Right ventricular remodeling induced by prolonged excessive endurance exercise is mediated by upregulating Wnt/ $\beta$ -catenin signaling in rats, *Int. J. Cardiol.* 413 (2024) 132316.
- [18] T. Radovits, A. Oláh, Á. Lux, et al., Rat model of exercise-induced cardiac hypertrophy: hemodynamic characterization using left ventricular pressure-volume analysis, *Am. J. Physiol. Heart Circ. Physiol.* 305 (2013) H124–H134.

- [19] A. Oláh, C. Mátyás, D. Kellermayer, et al., Sex differences in morphological and functional aspects of exercise-induced cardiac hypertrophy in a rat model, *Front. Physiol.* 10 (2019) 889.
- [20] B. Bódi, A. Oláh, L. Mártha, et al., Exercise-induced alterations of myocardial sarcomere dynamics are associated with hypophosphorylation of cardiac troponin I, *Rev. Cardiovasc. Med.* 22 (2021) 1079–1085.
- [21] A. Oláh, A. Kovács, Á. Lux, et al., Characterization of the dynamic changes in left ventricular morphology and function induced by exercise training and detraining, *Int. J. Cardiol.* 277 (2019) 178–185.
- [22] A. Pelliccia, B.J. Maron, A. Spataro, M.A. Proschan, P. Spirito, The upper limit of physiologic cardiac hypertrophy in highly trained elite athletes, *N. Engl. J. Med.* 324 (1991) 295–301.
- [23] Y. Wang, U. Wisloff, O.J. Kemi, Animal models in the study of exercise-induced cardiac hypertrophy, *Physiol. Res.* 59 (2010) 633–644.
- [24] J. Scharhag, G. Schneider, A. Urhausen, V. Rochette, B. Kramann, W. Kindermann, Athlete's heart: right and left ventricular mass and function in male endurance athletes and untrained individuals determined by magnetic resonance imaging, *J. Am. Coll. Cardiol.* 40 (2002) 1856–1863.
- [25] P. Bohm, G. Schneider, L. Linneweber, et al., Right and left ventricular function and mass in male elite master athletes: a controlled contrast-enhanced cardiovascular magnetic resonance study, *Circulation* 133 (2016) 1927–1935.
- [26] I. Shimizu, T. Minamino, Physiological and pathological cardiac hypertrophy, *J. Mol. Cell. Cardiol.* 97 (2016) 245–262.
- [27] A. Oláh, B.T. Németh, C. Mátyás, et al., Physiological and pathological left ventricular hypertrophy of comparable degree is associated with characteristic differences of in vivo hemodynamics, *Am. J. Physiol. Heart Circ. Physiol.* 310 (2016) H587–H597.
- [28] B. Domenech-Ximenes, M. Sanz-de la Garza, S. Prat-González, et al., Prevalence and pattern of cardiovascular magnetic resonance late gadolinium enhancement in highly trained endurance athletes, *J. Cardiovasc. Magn. Reson.* 22 (2020) 62.
- [29] S. Möhlenkamp, N. Lehmann, F. Breuckmann, et al., Running: the risk of coronary events : prevalence and prognostic relevance of coronary atherosclerosis in marathon runners, *Eur. Heart J.* 29 (2008) 1903–1910.
- [30] B. Benito, G. Gay-Jordi, A. Serrano-Mollar, et al., Cardiac arrhythmogenic remodeling in a rat model of long-term intensive exercise training, *Circulation* 123 (2011) 13–22.
- [31] Z. Rao, S. Wang, W.P. Bunner, Y. Chang, R. Shi, Exercise induced right ventricular fibrosis is associated with myocardial damage and inflammation, *Korean Circ. J.* 48 (2018) 1014–1024.
- [32] S.M. Abdullah, K.W. Barkley, P.S. Bhella, et al., Lifelong physical activity regardless of dose is not associated with myocardial fibrosis, *Circ. Cardiovasc. Imaging* 9 (2016).
- [33] O. Missenard, C. Gabaudan, H. Astier, F. Desmots, E. Garnotel, P.L. Massoure, Absence of cardiac damage induced by long-term intensive endurance exercise training: a cardiac magnetic resonance and exercise echocardiography analysis in masters athletes, *Am. J. Prev. Cardiol.* 7 (2021) 100196.
- [34] D. Mo, W. Tian, H.N. Zhang, et al., Cardioprotective effects of galectin-3 inhibition against ischemia/reperfusion injury, *Eur. J. Pharmacol.* 863 (2019) 172701.
- [35] M. Zulkifli, A.U. Okonkwo, V.M. Gohil, FDX1 is required for the biogenesis of mitochondrial cytochrome c oxidase in mammalian cells, *J. Mol. Biol.* 435 (2023) 168317.
- [36] E.J. Mercer, Y.F. Lin, L. Cohen-Gould, T. Evans, Hspb7 is a cardioprotective chaperone facilitating sarcomeric proteostasis, *Dev. Biol.* 435 (2018) 41–55.
- [37] R. Nechushtai, L. Rowland, O. Karmi, H.B. Marjault, T.T. Nguyen, S. Mittal, R. S. Ahmed, D. Grant, C. Manrique-Acevedo, F. Morcos, J.N. Onuchic, R. Mittler, CISD3/MiNT is required for complex I function, mitochondrial integrity, and skeletal muscle maintenance, *Proc. Natl. Acad. Sci. U. S. A.* 121 (2024) e2405123121.
- [38] R. Bartucci, A. Salvati, P. Olinga, Y.L. Boersma, Vanin 1: its physiological function and role in diseases, *Int. J. Mol. Sci.* 20 (2019) 3891.
- [39] K. Dominiak, L. Galganski, A. Budzinska, A. Woyda-Ploszczyca, J.A. Zoladz, W. Jarmuskiewicz, Effects of endurance training on the coenzyme Q redox state in rat heart, liver, and brain at the tissue and mitochondrial levels: implications for reactive oxygen species formation and respiratory chain remodeling, *Int. J. Mol. Sci.* 23 (2022) 896.
- [40] B.T. Xu, S.R. Wan, Q. Wu, et al., BDH1 overexpression alleviates diabetic cardiomyopathy through inhibiting H3K9bb-mediated transcriptional activation of LCN2, *Cardiovasc. Diabetol.* 24 (2025) 101.
- [41] L. Banks, Z. Sasson, M. Busato, J.M. Goodman, Impaired left and right ventricular function following prolonged exercise in young athletes: influence of exercise intensity and responses to dobutamine stress, *J. Appl. Physiol.* 2010 (108) (1985) 112–119.
- [42] D. Oxborough, R. Shave, D. Warburton, et al., Dilatation and dysfunction of the right ventricle immediately after ultraendurance exercise: exploratory insights from conventional two-dimensional and speckle tracking echocardiography, *Circ. Cardiovasc. Imaging* 4 (2011) 253–263.
- [43] E. Kasikcioglu, H. Ofiaz, H. Akhan, A. Kayserilioglu, Right ventricular myocardial performance index and exercise capacity in athletes, *Heart Vessels* 20 (2005) 147–152.
- [44] A. D'Andrea, L. Riegler, S. Morra, et al., Right ventricular morphology and function in top-level athletes: a three-dimensional echocardiographic study, *J. Am. Soc. Echocardiogr.* 25 (2012) 1268–1276.
- [45] P.J.M. Wijnker, A.M. Murphy, G.J.M. Stienen, J. van der Velden, Troponin I phosphorylation in human myocardium in health and disease, *Neth. Heart J.* 22 (2014) 463–469.
- [46] J. Layland, R.J. Solaro, A.M. Shah, Regulation of cardiac contractile function by troponin I phosphorylation, *Cardiovasc. Res.* 66 (2005) 12–21.
- [47] A. Oláh, B.A. Barta, A.A. Sayour, et al., Balanced intense exercise training induces atrial oxidative stress counterbalanced by the antioxidant system and atrial hypertrophy that is not associated with pathological remodeling or arrhythmogenicity, *Antioxidants (Basel)* (2021) 10.
- [48] A. Polyák, L. Topal, N. Zombori-Tóth, et al., Cardiac electrophysiological remodeling associated with enhanced arrhythmia susceptibility in a canine model of elite exercise, *Elife* (2023) 12.
- [49] L. Such, A.M. Alberola, L. Such-Miquel, et al., Effects of chronic exercise on myocardial refractoriness: a study on isolated rabbit heart, *Acta Physiol (Oxf.)* 193 (2008) 331–339.
- [50] J.N. Weiss, A. Garfinkel, H.S. Karagueuzian, et al., Perspective: a dynamics-based classification of ventricular arrhythmias, *J. Mol. Cell. Cardiol.* 82 (2015) 136–152.
- [51] K.N. Jew, M.C. Olsson, E.A. Mokolke, B.M. Palmer, R.L. Moore, Endurance training alters outward K<sup>+</sup> current characteristics in rat cardiocytes, *J. Appl. Physiol.* 2001 (90) (1985) 1327–1333.